



New Discoveries in Cold Rolling: Understanding Stress Distribution and Parameter Dependence for Faster, More Accurate Models

Francis Flanagan¹(✉), Doireann O’Kiely¹, Alison O’Connor²,
Mozhdeh Erfanian³, and Edward James Brambley^{3,4}

¹ Department of Mathematics and Statistics, University of Limerick,
Limerick, Ireland

{francis.flanagan,doireann.okiely}@ul.ie

² School of Engineering and Bernal Institute, University of Limerick,
Limerick, Ireland

alison.oconnor@ul.ie

³ School of Mathematics, University of Warwick, Coventry, UK

{mozhdeh.erfanian,e.j.brambley}@warwick.ac.uk

⁴ WMG, University of Warwick, Coventry, UK

Abstract. The finite element (FE) method is a powerful tool for simulating industrial metal forming processes such as metal rolling. FE allows users to estimate the stress distribution in the metal sheet during the rolling process. However, FE simulations do not allow for real-time online process control due to model complexity and computational time. This paper forms part of a large-scale research project aimed at designing a simple-but-accurate mathematical model that provides sufficiently precise results (compared to FE simulations) with faster computational timescales allowing for real-time process control. To validate the asymptotics-based mathematical model, an accurate FE model is required. In this paper, we give a detailed description of a quasi-static Abaqus/Explicit FE model and show how this is optimised to represent the rolling process. We report new insights gained from the FE simulations which can guide the development of simpler, faster mathematical models.

Keywords: FE · plasticity · elasticity

1 Introduction

In metal rolling, a sheet of metal is fed gradually between two rotating rollers. The rollers are held at a fixed separation that is less than the initial thickness of the sheet and act to permanently deform the sheet so that its thickness is reduced (see Fig. 1). The system considered in this paper is symmetric about the sheet centre, and the top roller rotates anti-clockwise so that the sheet moves in the positive x -direction. Metal rolling has been studied for decades, with some of the early slab-type mathematical models dating back as far as 1924 [19].

More than 95% of ferrous and non-ferrous metals and alloys are processed to their usable forms by rolling [17]. Given the importance of metal rolling processes, many authors have attempted to augment existing analytical models to account for variables such as through-thickness variations in stresses, displacements and velocities, which early slab models neglected [13]. Some models [2] contain systematic assumptions about the process, e.g., thin sheet and large roller. These assumptions enable an asymptotic analysis to be carried out. At leading order, slab theory is recovered, and at higher orders through-thickness variations are predicted. However, the accuracy of this updated asymptotic model is still under debate, as the influence of key phenomena such as residual stresses and elastic springback on asymptotic outputs remain unclear.

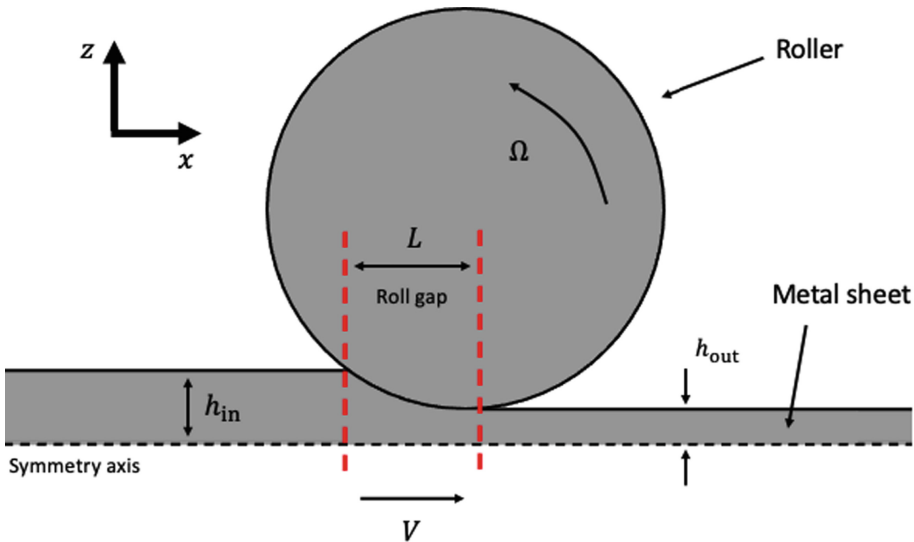


Fig. 1. Schematic of the metal rolling process. The sheet moves from left to right and its thickness is reduced by the roller. Symmetry about the centre of the sheet is assumed.

The FE method is a numerical technique that can be applied to solve a wide variety of problems in engineering and science governed by partial differential equations (PDEs) [8]. The domain of interest is discretized into small regions (elements), and the solution is approximated by a sum of basis functions on these elements. The governing PDEs are used to give a system of algebraic equations for the amplitude of the basis functions, and the resulting global solution converges to the exact solution of the PDEs as the size of the elements decreases.

The FE method provides a better understanding of the stress distribution in the metal sheet during the rolling process compared to exact solutions of the simplified slab model. However, a key limitation of FE modelling is that simulations take too long to allow for real-time online process control, with some FE rolling models taking hundreds of hours to run (e.g., [6]). Without real-time process control, most forming processes remain open loop and rely on

many repetitions to find viable operating conditions, producing large amounts of waste material [12]. For example, 640Mt of CO₂ per year is created globally from steel which is subsequently turned into scrap, approximately equivalent to 100 coal power stations [1]. Real-time process control would allow for monitoring the workpiece and correcting mistakes as they happen, as opposed to the current trial-and-error approach. This work is part of a large-scale project whose long-term goal is to derive models that are much simpler (giving faster computation times), but still accurate, using asymptotic methods. An accurate FE model is required both to drive the asymptotic analysis and to validate the resulting reduced model. The formation, optimisation and outputs of this FE model are the subject of this paper.

Section 2 describes the FE model used to simulate metal rolling and details the model formulation and validation to ensure a quasi-static approximation is achieved. In Sect. 3 oscillations in simulation results are discussed and a method of removing these high-frequency oscillations is proposed. We discuss the physical insights that can be gained from FE results in Sect. 4, such as the shape of the boundary between the plastic and elastic deformation zones in the sheet presented by the simulation results. In Sect. 5 we draw conclusions and briefly discuss some future plans for our FE simulations, which can guide the development of simpler, faster mathematical models.

2 Mathematical Model

As shown in Fig. 1, a relatively thin sheet of half-thickness $h_{\text{in}} = 0.005$ m (compared to roller radius $R = 0.1$ m) is considered. By assuming the metal sheet's width is much larger than its thickness, we can consider an idealised two-dimensional geometry by assuming plane-strain conditions apply [18]. We consider a sheet of elastic-plastic material, which deforms elastically up to some yield stress, above which it deforms plastically. The roller is assumed to be rigid, so no roller deformation occurs. We also exploit the symmetry of this particular metal rolling system about the centre of the metal sheet (see Fig. 1) and consider the top half of the sheet and the top roller only. These modelling choices reduce the computational intensity of the problem, and in turn facilitate the use of a finer mesh in the FE formulation.

In metal rolling processes, speeds are typically quite low, (approximately $1 \text{ m}\cdot\text{s}^{-1}$). Therefore inertia effects can be ignored and the rolling process can be idealised as quasi-static [3].

Three boundary conditions are applied in this analysis. First, the sheet's horizontal centre line (i.e., the symmetry axis in Fig. 1) is constrained vertically to enforce the expected symmetry. Second, the centre of the roller is held in a fixed position, so its only degree of freedom is rotation in the rolling direction. Finally, the roller is given an angular velocity of $\Omega = 6.283 \text{ rad}\cdot\text{s}^{-1}$. The sheet is also given an initial velocity of $R\Omega = 0.6283 \text{ m}\cdot\text{s}^{-1}$, roughly equal to the x -component of the roller's velocity, in order to reduce any jumps in velocity when the sheet meets the roller.

2.1 FE Method Implementation in Abaqus

A comprehensive literature review [4,6,9] showed Abaqus/Explicit to be the preferred choice in most cases for modelling metal rolling processes due to its efficiency and speed compared to the implicit solver used in Abaqus/Standard. In this work Abaqus/Explicit 2021 [3] is implemented. The explicit dynamic analysis implements an explicit integration rule using diagonal element mass matrices. The equations of motion for the body are integrated using the explicit central-difference integration rule, where the accelerations calculated at time t are used to calculate the velocity solution at time $t + \Delta t/2$, Eq. 1, and the displacement solution to time $t + \Delta t$, Eq. 2.

$$\dot{u}_{(i+\frac{1}{2})}^N = \dot{u}_{(i-\frac{1}{2})}^N + \frac{\Delta t_{(i+1)} + \Delta t_{(i)}}{2} \ddot{u}_{(i)}^N, \quad (1)$$

$$u_{(i+1)}^N = u_{(i)}^N + \Delta t_{(i+1)} \dot{u}_{(i+\frac{1}{2})}^N. \quad (2)$$

Here u^N is a degree of freedom (usually a displacement or a rotation component) and the subscript i refers to the increment number in an explicit dynamics step.

Quasi-static analyses typically have longer timescales which increase the numerical computation time required by FE methods. However, Abaqus/Explicit enables the use of mass-scaling. Mass scaling uniformly scales the density of the material within the simulation to facilitate longer time steps and, hence, reduce computational time [12]. This occurs since the stable time increment for Abaqus/Explicit simulations, which is the largest possible time step the solver can take without results becoming unstable, is related to the density of the material being analysed by

$$\Delta t_{\text{stable}} \approx \frac{L^e \sqrt{\rho}}{\sqrt{E}}, \quad (3)$$

where L^e is the length of an element, ρ is the material density and E is the Young's modulus of the material. The mass scaling factor (MSF) must be chosen carefully to reduce simulation times without introducing inertial effects, which can lead to erroneous and unstable outputs [7,11]. In this work, the MSF is chosen to be 2000 and this is considered a typical value for conducting quasi-static metal forming analyses with Abaqus/Explicit [11,14].

In FE analyses, the material model itself may provide damping in the form of plastic dissipation or viscoelasticity. For many applications such damping may be adequate. However, in some cases, it can be desirable to introduce some additional damping to provide another dissipation source. In this work we restrict our attention to stiffness-proportional Rayleigh damping. In stiffness-proportional damping, a damping stress, $\tilde{\sigma}_d$, is added to the stress caused by the constitutive response at the integration point when the dynamic equilibrium equations are formed, but it is not included in the stress output. This stress is given by

$$\tilde{\sigma}_d = \beta \tilde{D}^{el} \dot{\epsilon}, \quad (4)$$

where β is the stiffness-proportional damping factor, \tilde{D}^{el} is the current elastic stiffness and $\dot{\epsilon}$ is the strain rate. Stiffness-proportional damping must be used

with caution because it may significantly reduce the stable time increment. To avoid a dramatic drop in the stable time increment, β should be less than or of the same order of magnitude as the initial stable time increment without damping [3].

In order to implement the model assumptions discussed earlier, the metal sheet and roller are modelled as a 2D shell planar part and as a 2D analytical rigid part respectively. To adhere to the plane-strain assumption, linear quadrilateral plane-strain elements with reduced integration (i.e., type CPE4R) are used here. Only one roller and half the sheet's thickness is modelled because of the assumption of symmetry about the sheet's horizontal centre line.

For the FE simulations in this paper, the global mesh element size and the stiffness-proportional material damping factor, β , are analysed to investigate their effect on oscillations in the FE simulations, as we will see in Sect. 3. Table 1 shows the name, element size and β value for each simulation. The physical parameters given here and in each figure caption remain unchanged for each simulation: $(h_{\text{in}}, R, r, \rho, E, \nu, \sigma_y, \hat{\mu}) = (0.005, 0.1, 0.2, 7850, 1.5 \times 10^{11}, 0.35, 3 \times 10^8, 0.1)$, where h_{in} is the initial sheet half-thickness and R is the roller radius, which both have units of m, r is the sheet reduction fraction, ρ is the density of the metal sheet with units of $\text{kg}\cdot\text{m}^{-3}$, E is the Young's modulus with units of Pa, ν is Poisson's ratio, σ_y is the yield stress of the metal, measured in Pa, and $\hat{\mu}$ is the friction coefficient between the roller and the sheet. Values of the friction coefficient for industrial cold rolling mills are usually in a range of approximately $\hat{\mu} = 0.02 - 0.15$ [10]. The rest of these parameter and geometry values are common values for industrial cold metal rolling of steel sheets (as stated in [2]).

Table 1. Table showing the name, element size and material damping factor (β) of each simulation considered in this paper. The physical parameters used in all simulations are given by $(h_{\text{in}}, R, r, \rho, E, \nu, \sigma_y, \hat{\mu}) = (0.005, 0.1, 0.2, 7850, 1.5 \times 10^{11}, 0.35, 3 \times 10^8, 0.1)$.

Simulation name	Mesh element size	Damping factor (β)
S1	5×10^{-5} m	0
S2	10×10^{-5} m	0
S3	20×10^{-5} m	0
S4	40×10^{-5} m	0
S5	5×10^{-5} m	2.5×10^{-7} s

2.2 Verification of Quasi-static Behaviour

If a simulation is truly quasi-static, the work applied by the external forces is nearly equal to the internal energy of the system. Also, the inertial forces should be negligible in a quasi-static analysis because the velocity of the material in the model is very small. The corollary to both of these conditions is that the kinetic energy of the deforming material should not exceed a small fraction (typically 5–10%) of its internal energy throughout most of the process [3, 15].

Figure 2 shows the typical ratio between the kinetic energy and the internal strain energy (KE/IE) for the whole system for the simulations considered in this paper. It should be noted that the value of the MSF (which is 2000 for all simulations in this paper) is acceptable since the energy ratio is between 5% and 10% for the majority of each simulation. For example, we can see in Fig. 2 that after roughly 0.08 roller rotations, the energy ratio dips below 10%, and therefore we can say that the FE simulations are in a quasi-static state, since the rule of thumb is satisfied throughout most of the process. It is not expected that this condition is satisfied at the early stages of the simulations [14]. This rule is followed for all simulations considered in this paper.

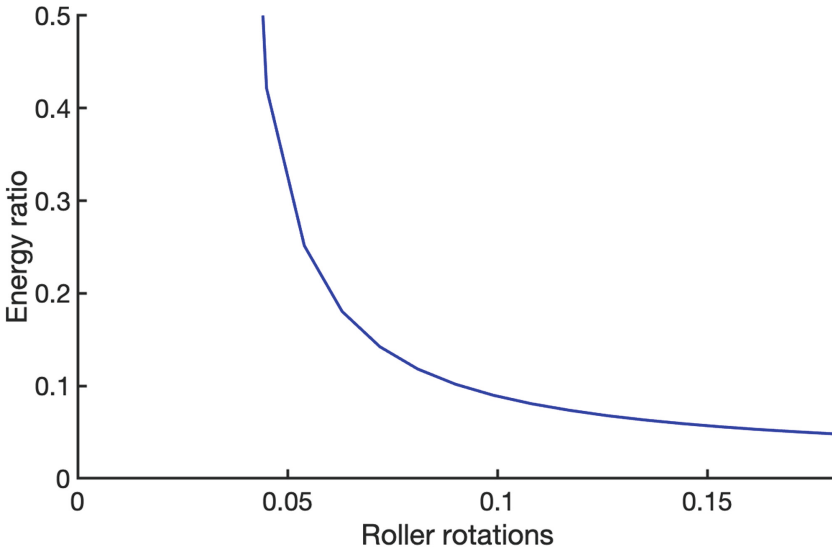


Fig. 2. Typical ratio between the kinetic energy and the internal strain energy (KE/IE) for the whole rolling system for the simulations considered in this paper. The vertical axis is limited to 0.5 since negligible internal energy caused a spike in this ratio at early stages of the simulation. The physical parameters used in all simulations are given by $(h_{in}, R, r, \rho, E, \nu, \sigma_y, \hat{\mu}) = (0.005, 0.1, 0.2, 7850, 1.5 \times 10^{11}, 0.35, 3 \times 10^8, 0.1)$.

3 Results

During initial simulations, high-frequency oscillations were observed near the surface of the sheet between $x = 0$ and $x = 0.4$ (see Fig. 3(a) and Fig. 3(b)). To investigate whether these oscillations are a numerical artefact or are representative of an intrinsic physical property, we monitor the effect of the mesh size and material damping on simulation results and analyse their influence on the size and existence of these oscillations in this section.

It should be noted that for every results figure presented in this paper, all of the quantities are scaled with representative values for visualization, making

all plots dimensionless. For example, x is scaled with the horizontal length of the roll gap L , so that $x = 0$ and $x = 1$ correspond to the start and end of the roll gap respectively in all figures. Similarly, z is scaled with the initial half-thickness of the sheet h_{in} , so that $z = 0$ and $z = 1$ correspond to the centre and undeformed surface of the sheet respectively. The vertical velocity v_z is scaled with $(R\Omega h_{\text{in}})/L$ and all stress quantities are scaled with the yield stress σ_y .

3.1 Mesh Density

Figure 3 shows three contour plots of the dimensionless vertical velocity v_z for the simulations S1, S3 and S5 respectively. Oscillations are illustrated in both Fig. 3(a) and Fig. 3(b) near the surface of the sheet between $x = 0$ and $x = 0.4$ approximately. It should be noted that these oscillations are present in contour plots of other quantities (v_x and σ_{xy} for example), but for brevity, only v_z results are investigated in this paper with regards to these oscillations. One possibility is that the oscillations are numerical artefacts and can simply be filtered away when post-processing the results. This is the hypothesis we want to check by varying the mesh density to see what happens to these oscillations.

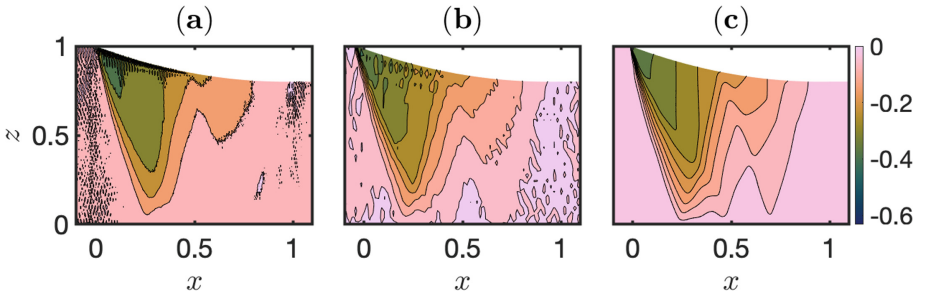


Fig. 3. Contour plot of dimensionless vertical velocity v_z in a metal sheet with material properties $(h_{\text{in}}, R, r, \rho, E, \nu, \sigma_y, \hat{\mu}) = (0.005, 0.1, 0.2, 7850, 1.5 \times 10^{11}, 0.35, 3 \times 10^8, 0.1)$, for the simulations (a) S1, (b) S3 and (c) S5 in Table 1. The dimensions of the sheet are normalized so that $x = 0$ and $x = 1$ correspond to the start and end of the sheet respectively, and so that $z = 0$ and $z = 1$ correspond to the sheet centre line and top undeformed surfaces respectively. Symmetry about the centre of the sheet is assumed, and so only the top half of the sheet is displayed here. The numerical oscillations observed between $x = 0$ and $x = 0.4$ in both Fig. 3(a) and Fig. 3(b) are not visible in Fig. 3(c).

As we can see from both Fig. 3(a) and Fig. 3(b), the region of space occupied by the oscillations seems to scale with the mesh size. For the simulation S1 (with mesh size 5×10^{-5} m) these oscillations take up much less space than for the simulation S3 (with mesh size 20×10^{-5} m). This suggests that the oscillations are numerical artefacts, but it is not conclusive. We investigate further by assessing the amplitude of the oscillations. We use linear interpolation to extract the vertical velocity, v_z , at different values of the thickness position z for $x = 0.2$, inside

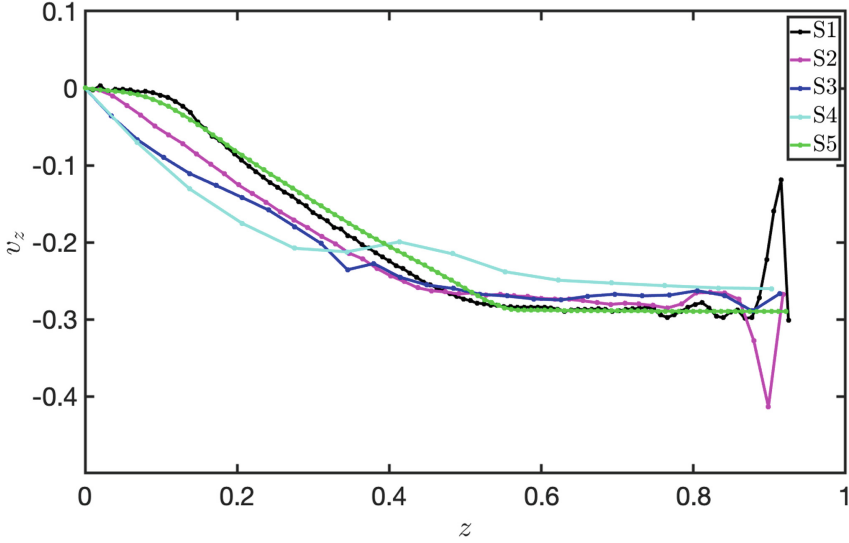


Fig. 4. Dimensionless vertical velocity v_z as a function of height z in a cross-section $x = 0.2$ for all simulations in Table 1. The physical parameters used in all simulations are given by $(h_{\text{in}}, R, r, \rho, E, \nu, \sigma_y, \hat{\mu}) = (0.005, 0.1, 0.2, 7850, 1.5 \times 10^{11}, 0.35, 3 \times 10^8, 0.1)$. The surface of the sheet corresponds to $z \approx 0.9$, where we can see high-amplitude oscillations, particularly for the two simulations with the finest mesh densities (5×10^{-5} m and 10×10^{-5} m).

the zone $x \in [0, 0.4]$ where the oscillations appear. These results are displayed in Fig. 4.

We observe that the oscillation amplitude increases as the mesh density increases (S4–S1), so the numerical solution does not converge. Additionally S4 fails to capture the oscillations seen in the other, more densely-meshed simulations (S1–S3). Despite the oscillatory behaviour of the finely-meshed simulations, a refined mesh is one of the principal means to ensure calculation accuracy [16]. Comparing S1 (fine mesh) with S4 (coarse mesh) we see poor agreement through the sheet thickness. This indicates that the mesh strategy used in S4 is not adequately refined. Therefore, it was concluded that coarsening the mesh was not a viable solution for removing these oscillations and that a fine mesh is needed, along with some other parameter change.

3.2 Material Damping

As stated earlier, the value of the damping factor, β , should be less than or of the same order of magnitude as the initial stable time increment without damping. The stable time increment for the simulation with mesh density 5×10^{-5} m and no damping (i.e., S1 in Table 1) is $\Delta t_{\text{stable}} = 2.547 \times 10^{-7}$ s, and so for preliminary investigations, a value of $\beta = 2.5 \times 10^{-7}$ s was trialled to see what effect, if any, this had on the oscillatory nature of the FE results near the surface of the sheet.

Comparing Fig. 3(c) to Fig. 3(a) and Fig. 3(b), we can see that the damped simulation S5 is free of the oscillations observed for S1 and S3 near the surface of the sheet. The additional damping stress added to the stress caused by the constitutive response successfully cleared away the oscillatory behaviour observed in simulations S1–S3. The question remains as to how much the material damping has influenced the resulting FE output. We investigate further by assessing the amplitude of the oscillations as a function of material damping. Again, we use linear interpolation to extract the value of v_z at different values of z along the line $x = 0.2$ for simulation S5.

In Fig. 4, we see that the damped simulation (S5) results capture the underlying behaviour of the undamped, finely-meshed simulation (S1) quite well throughout most of the thickness of the sheet, while smoothing the oscillatory behaviour. However, it should be noted that the CPU time required for simulation S5 was considerably higher than that for S1 (approximately 700 h compared to approximately 10 h). This comparison is therefore just a starting point for obtaining a suitable β value that provides a balance between practical computational time and successful implementation of material damping. This will be considered in future work.

4 Physical Insights

Figure 5 shows FE results from simulation S1 in Table 1. Figure 5(a) shows a dimensionless contour plot of the von Mises stress quantity and Fig. 5(b) shows dimensionless slip lines (which correspond to the maximum shear stress trajectories [20]).

Since plastic deformation only occurs when the von Mises stress is at or above the effective yield stress (in Fig. 5(a), this corresponds to the von Mises value of 1 since we have divided all stresses by the yield stress), and elastic deformation occurs below this value, Fig. 5(a) provides us with a picture of the shape of the boundary between the plastic and elastic zones within the metal sheet. In reduced asymptotics-based models (e.g., [2]) it is assumed that the plastic deformation zone starts where the sheet and roller first meet at $x = 0$ and that this zone is bounded to the left by a straight line at $x = 0$ throughout the thickness of the sheet. The same is assumed for the right-hand boundary at $x = 1$. However we see in Fig. 5(a) that these boundaries are not vertical lines at $x = 0$ or at $x = 1$. This computational result has been quite informative for building our mathematical model because now we can allow for some variation in the z -direction when writing down boundary conditions for our model, i.e., the boundary is now described by $x = x_t(z)$ instead of $x = 0$ at the roll gap entrance. We describe $x_t(z)$ as a “transition curve” where the sheet transitions from elastic to plastic behaviour. In the asymptotic limit where the aspect ratio ε is small, we expect $x_t(z)$ to have an $O(\varepsilon)$ deviation from vertical.

It is also worth noting that the entrance and exit boundary shapes are noticeably distinct and although it was hypothesised that one region would be a mirror image of the other, it looks as though careful consideration will have to be given to two separate problems; the entrance-region problem and the exit-region problem.

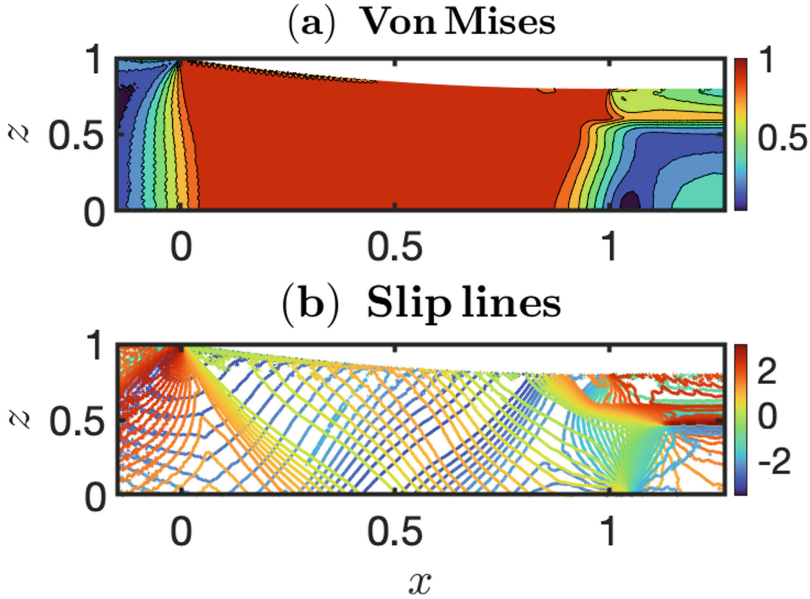


Fig. 5. Dimensionless FE results from simulation S1 in Table 1. Plot (a) shows a contour plot of von Mises stress and (b) a slip-line graph for a metal sheet with material properties $(h_{in}, R, r, \rho, E, \nu, \sigma_y, \hat{\mu}) = (0.005, 0.1, 0.2, 7850, 1.5 \times 10^{11}, 0.35, 3 \times 10^8, 0.1)$. The dimensions of the sheet are normalized so that $x = 0$ and $x = 1$ correspond to the start and end of the roll gap respectively, and so that $z = 0$ and $z = 1$ correspond to the sheet centre line and top undeformed surface respectively. Symmetry about the centre of the sheet is assumed, and so only the top half of the sheet is displayed here. These results are reproduced in companion paper [5].

Figure 5(b) is created by calculating the lines of maximum shear stress. The presence of oscillations in these shear slip lines and other quantities along the length of the roll gap necessitates wave-like solutions for the asymptotic problem, the details of which can be found in [5].

Finally, an interesting observation from both Fig. 5(a) and Fig. 5(b) is that the slip lines on the exit side of the roll gap (near $x = 1$) accumulate within a thin layer under the surface of the sheet, which roughly lines up with the region where a lot of residual stress is observed in the von Mises plot. These type of FE results can help in designing a simple-but-accurate mathematical model that provides sufficiently precise results (compared to FE simulations) with faster computational timescales. This model is described by Erfanian et al. in [5].

5 Conclusion

FE modelling is a highly influential method for simulating metal rolling. However, simulations often require large CPU hours to complete, and so FE analysis

is not a feasible approach for real-time online process control. If optimised correctly, asymptotics-based mathematical models could prove useful for online control, given their quick-to-compute nature, and potential to give accurate results when compared to FE simulations. This mathematical method often requires consideration of small or large parameters to simplify the governing equations to be solved. In metal rolling, this is often the aspect ratio (i.e., the horizontal length of the contact zone between the sheet and the roller is much longer than the initial half-thickness of the sheet itself). The FE method can act as a useful benchmark for comparisons against ever-developing mathematical models, but can also provide insight into the required setup of a mathematical model ahead of time.

We discuss here about the general modelling assumptions that make the FE and mathematical analysis simpler to conduct. The FE method implementation in Abaqus/Explicit is outlined, including details on how the model is confirmed to be in a quasi-static state.

Oscillatory behaviour was observed in the FE outputs near the surface of the metal sheet in preliminary results. The effects of mesh density and material damping on these oscillations is analysed and it is observed that a fine mesh with material damping is a suitable strategy for removing the high-frequency oscillations. However, the amount of damping required to keep CPU time at a minimum while still removing these oscillations is still not known and will have to be considered in future analyses.

Finally, physical insights gained from FE simulation results are briefly described that can help to guide the mathematical model formulation in the form of altering boundary condition definitions and inspiring wave-like solutions to be considered.

Acknowledgements. This publication has emanated from research conducted with the financial support of Science Foundation Ireland under Grant number 18/CRT/6049. For the purpose of Open Access, the author has applied a CC BY public copyright licence to any Author Accepted Manuscript version arising from this submission.

Dr O'Connor is funded by the European Union through the Marie Skłodowska-Curie Actions grant number 101028291. Mozhdeh Erfanian gratefully acknowledges the funding of a University of Warwick Chancellor's Scholarship. Edward James Brambley is grateful for the UKRI Future Leaders' Fellowship funding (MR/V02261X/1) supporting this work.

References

1. Allwood, J.M., et al.: Sustainable Materials: with Both Eyes Open, vol. 2012. UIT Cambridge Limited, Cambridge (2012)
2. Cawthorn, C., Minton, J., Brambley, E.: Asymptotic analysis of cold sandwich rolling. *Int. J. Mech. Sci.* **106**, 184–193 (2016)
3. Dassault Systèmes: SIMULIA User Assistance 2020 Abaqus (2020)
4. Edberg, J., Lindgren, L.E.: Efficient three-dimensional model of rolling using an explicit finite-element formulation. *Commun. Numer. Methods Eng.* **9**(7), 613–627 (1993)

5. Erfanian, M., Brambley, E., Flanagan, F., O'Kiely, D., O'Connor, A.: New models for cold rolling: generalized slab theory and slip lines for fast predictions without finite elements (2023)
6. Gavallas, E., Pressas, I., Papaefthymiou, S.: Mesh sensitivity analysis on implicit and explicit method for rolling simulation. *Int. J. Struct. Integrity* **9**(4), 465–474 (2018)
7. Ktari, A., Antar, Z., Haddar, N., Elleuch, K.: Modeling and computation of the three-roller bending process of steel sheets. *J. Mech. Sci. Technol.* **26**, 123–128 (2012)
8. Lenggana, B.W., et al.: Effects of mechanical vibration on designed steel-based plate geometries: behavioral estimation subjected to applied material classes using finite-element method. *Curved Layered Struct.* **8**(1), 225–240 (2021)
9. Lindgren, L.E., Edberg, J.: Explicit versus implicit finite element formulation in simulation of rolling. *J. Mater. Process. Technol.* **24**, 85–94 (1990)
10. Mang, T., et al.: *Encyclopedia of Lubricants and Lubrication*, vol. 1. Springer, Heidelberg (2014). <https://doi.org/10.1007/978-3-642-22647-2>
11. Min, W., He, Y., Sun, Z.C., Guo, L.G., Ou, X.Z.: Dynamic explicit FE modeling of hot ring rolling process. *Trans. Nonferrous Met. Soc. China* **16**(6), 1274–1280 (2006)
12. Minton, J.J.: *Mathematical modelling of asymmetrical metal rolling processes*. Ph.D. thesis, University of Cambridge (2017)
13. Minton, J., Cawthorn, C., Brambley, E.: Asymptotic analysis of asymmetric thin sheet rolling. *Int. J. Mech. Sci.* **113**, 36–48 (2016)
14. Natário, P., Silvestre, N., Camotim, D.: Web crippling failure using quasi-static FE models. *Thin-Walled Struct.* **84**, 34–49 (2014)
15. Prior, A.: Applications of implicit and explicit finite element techniques to metal forming. *J. Mater. Process. Technol.* **45**(1–4), 649–656 (1994)
16. Qian, X., Chengguo, W., Ge, G.: The research of parallel computing for large-scale finite element model of wheel/rail rolling contact. In: 2010 3rd International Conference on Computer Science and Information Technology, vol. 1, pp. 254–257. IEEE (2010)
17. Ray, S.: *Principles and Applications of Metal Rolling*. Cambridge University Press, Cambridge (2016)
18. Richelsen, A.B.: Comparison of a numerical analysis of rolling with experimental data. *J. Mater. Process. Technol.* **57**(1–2), 70–78 (1996)
19. Smet, R.P., Johnson, R.E.: An asymptotic analysis of cold sheet rolling. *J. Appl. Mech.* **56**, 33–39 (1989)
20. Tapponnier, P., Molnar, P.: Slip-line field theory and large-scale continental tectonics. *Nature* **264**(5584), 319–324 (1976)